2021 IEEE International Conference on Communications Workshops (ICC Workshops) | 978-1-7281-9441-7/20/$31.00 ©2021 IEEE | DOI: 10.1109/ICCWorkshops50388.2021.9473656

Robust Max-Min Fair Beamforming of Secrecy SWIPT IoT Systems Under a Non-Linear EH Model

Zhengyu Zhu†, Zixuan Wang⋆†, Yu Lin†, Peijia Liu†, Wanming Hao†, Zhongyong Wang†, Inkyu Lee‡
† School of Information Engineering, Zhengzhou University, China
⋆ Ningxia key Laboratory for Photovoltaic Materials, Ningxia University, China
‡ School of Electrical Engineering, Korea University, Korea
Email: zhuzhengyu6@gmail.com, iezywang@zzu.edu.cn, inkyu@korea.ac.kr

***Abstract*—In this paper, we study a robust beamforming design for multi-user multiple-input multiple-output secrecy networks with simultaneous wireless information and power transfer (SWIPT). In this system, an access point, multiple Internet of Things devices under the non-Linear energy harvesting model with a help of one cooperative jammer (CJ). We employ artificial noise (AN) generation to facilitate efficient wireless energy transfer and secure transmission. To achieve energy harvesting fairness, we aim to maximize the minimum harvested energy among users subject to secrecy rate constraint and total transmit power constraint in the presence of channel estimation errors. By incorporating a norm-bounded channel uncertainty model, we propose an algorithm based on sequential parametric convex approximation (SPCA). Finally, simulation results show that the proposed SPCA method outperforms the traditional AN-aided method and CJ-aided method.**

***Index Terms*—SWIPT, non-Linear energy harvesting, CJ, norm-bounded channel uncertainty model, SPCA.**

I. Introduction

The fifth generation (5G) wireless systems are expected to meet an continuously increasing demand for wireless applications such as wide radio coverage and high data rate [1]. Due to the advancement of wireless sensor networks (WSNs) and Internet of Things (IoT), the energy-constrained 5G network needs support millions of intelligent terminals.One main research approach in wireless power transfer (WPT) is the SWIPT technigue [2], which has attracted a lot of interests for providing power supplies for wireless IoT networks [3]-[6].

On the other hand, secrecy transmission has extracted attentions in communication systems [7] [8]. Specifically, physical-layer security (PLS) has been recognized as an important issue for SWIPT systems since the wireless information is more vulnerable to eavesdropping [9] [10].

Another aspect that we address in this paper is the impact of imperfect channel state information (CSI). In practice, it is not always possible to obtain perfect CSI at the transmitter due to channel estimation errors [11] [12]. Secure communication with SWIPT would be more challenging in the presence of the imperfect CSI [13]-[19].

In addition, artificial noise (AN) methods have been used by embedding the transmit beamforming to confuse eavesdroppers [7]. In secrecy SWIPT systems, the AN plays the roles of both carrying an energy signal for WPT and protecting the secrecy information transmission [20]. Also, to further increase the secrecy performance, a jamming node has been introduced in the secrecy networks, which prevents the eavesdroppers from intercepting the intended messages [14]-[16]. When information receivers (IRs) and energy harvesting receivers (ERs) are placed in a same cell, the ERs are normally assumed to be closer to the transmitter compared with IRs due to its low power sensitivity level. In such a situation, the ERs have a possibility of eavesdropping the information sent to the IRs, and thus can become potential eavesdroppers [13].

In this paper, we investigate a secure transmission design problem in a MU-MIMO secrecy IoT system with SWIPT. In this system, a multi-antenna transmitter supports single-antenna co-located receiver (CR) IoT nodes, and multi-antenna EH IoT nodes in the presence of a multi-antenna CJ. Unlike the work in [10], our objective is to maximize the minimum harvested energy of both EH nodes and CR nodes subject to secrecy rate constraints and the total transmit power constraint by incorporating the norm-bounded channel uncertainty model.

Moreover, we seek a transmission strategy to jointly design the AN-aided beamforming matrix, the AN covariance matrix, the jamming covariance matrix and the PS ratio. Then, an iterative algorithm based on SPCA is also addressed, where the original problem is transformed to a second order cone programming (SOCP) problem that can be directly solved by CVX. Finally, Simulation results demonstrate that the proposed SPCA scheme outperforms the traditional methods.

II. System Model

A. Network Model

We consider a secure downlink MU-MIMO SWIPT-based IoT system as shown in Fig. 1, which consists of one transmitter, one CJ, K CR nodes, and L EH nodes. Here the CR node employs the PS scheme to decode information and harvest power simultaneously. It is assumed that the transmitter, the CJ and the EH node are equipped with N_T, N_J and N_E antennas,

This work was supported in part by the National Natural Science Foundation of China under Grant 61801434, 61801435 and 61771431, in part by the Science and Technology Innovation Project of Zhengzhou under Grant 2019CXZX0037, in part by the National Key Research and Development Program of China under Grant 2019YFB1803200, in part by the National Research Foundation (NRF) through the Ministry of Science, ICT, and Future Planning (MSIP), Korea Government under Grant 2017R1A2B3012316. Corresponding Author: Peijia Liu.

respectively, while CR nodes have a single antenna. We denote $\mathbf{h}_{s,k} \in \mathbb{C}^{N_T}$ as the channel vector between the transmitter and the k-th CR node, $\mathbf{H}_{e,l} \in \mathbb{C}^{N_T \times N_E}$ as the channel matrix between the transmitter and the l-th EH node, $\mathbf{g}_{s,k} \in \mathbb{C}^{N_J}$ as the channel vector between the CJ and the k-th CR node, $\mathbf{G}_{e,l} \in \mathbb{C}^{N_J \times N_E}$ as the channel matrix between the CJ and the l-th EH node, respectively.

The transmitter sends the message $\mathbf{x}_k$ to the k-th CR node as

$$\mathbf{x}_k = \mathbf{f}_k s_k + \mathbf{z}, \tag{1}$$

where $\mathbf{f}_k \in \mathbb{C}^{N_T}$ indicates the linear beamforming vector for the k-th CR node at the transmitter, $s_k \in \mathcal{C}$ represents the information-bearing signal intended for the k-th CR node with $\mathbb{E}\{|s_k|^2\} = 1$, and $\mathbf{z} \in \mathbb{C}^{N_T}$ is the energy-carrying AN vector, which can also be composed by multiple energy beams.

The received signal at the k-th CR node and the l-th EH node can be expressed as

$$\begin{aligned} y_{s,k} &= \mathbf{h}_{s,k}^H \sum_{k=1}^{K} \mathbf{f}_k s_k + \mathbf{h}_{s,k}^H \mathbf{z} + \mathbf{g}_{s,k}^H \mathbf{q} s_J + n_{s,k}, \ k = 1, ..., K, \\ \boldsymbol{y}_{e,l} &= \mathbf{H}_{e,l}^H \sum_{k=1}^{K} \mathbf{f}_k s_k + \mathbf{H}_{e,l}^H \mathbf{z} + \mathbf{G}_{e,l}^H \mathbf{q} s_J + \mathbf{n}_{e,l}, \ l = 1, ..., L, \end{aligned} \tag{2}$$

where $\mathbf{q} \in \mathbb{C}^{N_J}$ indicates the CJ vector, s_J equals the cooperative jamming signal introduced by the CJ with $\mathbb{E}\{|s_J|^2\} = 1$, and $n_{s,k} \sim \mathcal{CN}(0, \sigma_{s,k}^2)$ and $\mathbf{n}_{e,l} \sim \mathcal{CN}(0, \sigma_{e,l}^2 \mathbf{I})$ stand for the additive Gaussian noise at the k-th CR node and the l-th EH node, respectively.

The received signal at the k-th CR node is divided into the ID and EH parts by the PS ratio $\rho_{s,k} \in (0, 1]$. Thus, the received signal for ID at the k-th CR node can be given as

$$\begin{aligned} y_{s,k}^{ID} &= \sqrt{\rho_{s,k}} y_{s,k} + n_{p,k} \\ &= \sqrt{\rho_{s,k}} \left(\mathbf{h}_{s,k}^H \sum_{k=1}^{K} \mathbf{f}_k s_k + \mathbf{h}_{s,k}^H \mathbf{z} + \mathbf{g}_{s,k}^H \mathbf{q} s_J + n_{s,k} \right) + n_{p,k}, \end{aligned} \tag{3}$$

where $n_{p,k} \sim \mathcal{CN}(0, \sigma_{p,k}^2)$ is the noise at the k-th CR node [2].

Let us define $\mathbf{F}_k = \mathbf{f}_k \mathbf{f}_k^H$ as the transmit covariance matrix, $\mathbf{Z} = \mathbf{z}\mathbf{z}^H$ as the AN covariance matrix, and $\mathbf{Q} = \mathbf{q}\mathbf{q}^H$ as the CJ covariance matrix. Hence, the achieved secrecy rate can be calculated by

$$\hat{R}_{s,k} = \left[C_{s,k}(\rho_{s,k}, \mathbf{F}_k, \mathbf{Z}, \mathbf{Q}) - \max_l C_{l,k}(\rho_{s,k}, \mathbf{F}_k, \mathbf{Z}, \mathbf{Q}) \right]^+, \tag{4}$$

where $C_{s,k}$ and $C_{l,k}$ are defined in (5) on the top of the next page.

B. Non-linear EH model

As mentioned previously, linear EH model is mostly used in SWIPT system, and the harvested energy is given by

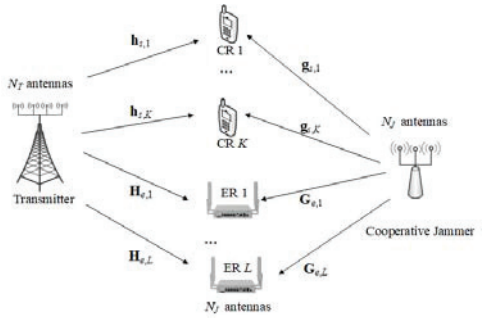

Fig. 1. System model of secure SWIPT IoT systems with cooperative jamming for MU-MIMO downlink.

$\Phi = \eta P_{in}$, where P_{in} represents the input power at the receiver, and $\eta \in [0, 1]$ is the energy conversion efficiency [17] [18]. However, the practical EH circuits exhibit nonlinear EH behavior due to the saturation of the rectifier. To avoid the mismatch caused by the linear EH model, we employ the logistic-function based nonlinear EH model, as

$$\Phi^{prac}(P_{in}) = \frac{\frac{M_i}{1+\exp(-a_i(P_{in}-b_i))} - \frac{M_i}{1+\exp(a_i b_i)}}{1 - \frac{1}{1+\exp(a_i b_i)}}, \tag{6}$$

where M_i is a constant expressing the maximum harvested power at the i-th CR/ER node when EH circuit reaches saturation. Parameters a_i and b_i are also constants in connection with the detailed circuit specifications, as defined in [21].

Using the non-linear EH model, the harvested power at the k-th CR node and the l-th EH node is expressed as

$$E_{s,k}^{prac} = \Phi^{prac}(E_{s,k}), \forall k, \qquad E_{e,l}^{prac} = \Phi^{prac}(E_{e,l}), \ \forall l. \tag{7}$$

where

$$\begin{aligned} E_{s,k} &= (1-\rho_{s,k}) \left(\mathbf{h}_{s,k}^H \Big(\sum_{k=1}^{K} \mathbf{F}_k + \mathbf{Z} \Big) \mathbf{h}_{s,k} + \mathbf{g}_{s,k}^H \mathbf{Q} \mathbf{g}_{s,k} + \sigma_{s,k}^2 \right), \\ E_{e,l} &= \mathrm{tr}(\mathbf{H}_{e,l}^H (\sum_{k=1}^{K} \mathbf{F}_k + \mathbf{Z}) \mathbf{H}_{e,l}) + \mathrm{tr}(\mathbf{G}_{e,l}^H \mathbf{Q} \mathbf{G}_{e,l}) + N_E \sigma_{e,l}^2. \end{aligned} \tag{8}$$

III. Problem Formulation and Robust Design Methods

In this paper, our goal is to jointly optimize the worst-case formulation assuming imperfect CSI. Adopting the norm-bounded channel uncertainty model [13], the actual channels $\mathbf{h}_{s,k}$, $\mathbf{H}_{e,l}$, $\mathbf{g}_{s,k}$, and $\mathbf{G}_{e,l}$ can be given as

$$\begin{aligned} \mathbf{h}_{s,k} &= \bar{\mathbf{h}}_{s,k} + \mathbf{e}_{s,k}, \forall k, \quad \mathbf{H}_{e,l} = \bar{\mathbf{H}}_{e,l} + \mathbf{E}_{e,l}, \forall l, \\ \mathbf{g}_{s,k} &= \bar{\mathbf{g}}_{s,k} + \tilde{\mathbf{e}}_{s,k}, \forall k, \quad \mathbf{G}_{e,l} = \bar{\mathbf{G}}_{e,l} + \tilde{\mathbf{E}}_{e,l}, \forall l, \end{aligned} \tag{9}$$

where $\bar{\mathbf{h}}_{s,k}, \bar{\mathbf{g}}_{s,k}, \bar{\mathbf{H}}_{e,l}$, and $\bar{\mathbf{G}}_{e,l}$ denote the estimated channel at the transmitter and the CJ, and $\mathbf{e}_{s,k}, \tilde{\mathbf{e}}_{s,k}, \mathbf{E}_{e,l}$, and $\tilde{\mathbf{E}}_{e,l}$ are the channel errors bounded as $\|\mathbf{e}_{s,k}\|_2 \le \varepsilon_{s,k}$, $\|\tilde{\mathbf{e}}_{s,k}\|_2 \le \tilde{\varepsilon}_{s,k}$, $\|\mathbf{E}_{e,l}\|_F \le \varepsilon_{e,l}$, and $\|\tilde{\mathbf{E}}_{e,l}\|_F \le \tilde{\varepsilon}_{e,l}$.

$$C_{s,k}(\rho_{s,k},\mathbf{F}_k,\mathbf{Z},\mathbf{Q})=\log_2\left(1+\frac{\rho_{s,k}\mathbf{h}_{s,k}^H\mathbf{F}_k\mathbf{h}_{s,k}}{\rho_{s,k}(\sigma_{s,k}^2+\sum_{j\neq k}\mathbf{h}_{s,k}^H\mathbf{W}_j\mathbf{h}_{s,k}+\mathbf{h}_{s,k}^H\mathbf{Z}\mathbf{h}_{s,k}+\mathbf{g}_{s,k}^H\mathbf{Q}\mathbf{g}_{s,k})+\sigma_{p,k}^2}\right),$$
$$C_{l,k}(\rho_{s,k},\mathbf{F}_k,\mathbf{Z},\mathbf{Q})=\log_2\left|\mathbf{I}+(\mathbf{H}_{e,l}^H\mathbf{Z}\mathbf{H}_{e,l}+\mathbf{G}_{e,l}^H\mathbf{Q}\mathbf{G}_{e,l}+\sigma_{e,l}^2\mathbf{I})^{-1}\mathbf{H}_{e,l}^H\mathbf{F}_k\mathbf{H}_{e,l}\right|. \tag{5}$$

$$\max_{\rho_{s,k},\{\mathbf{F}_k\},\mathbf{Z},\mathbf{Q}}\quad\left(\min_{\|\mathbf{e}_{s,k}\|\le\varepsilon_{s,k},\|\tilde{\mathbf{e}}_{s,k}\|\le\tilde{\varepsilon}_{s,k}}E_{s,k}^{prac}+\min_{\|\mathbf{E}_{e,l}\|_F\le\varepsilon_{e,l},\|\tilde{\mathbf{E}}_{e,l}\|_F\le\tilde{\varepsilon}_{e,l}}E_{e,l}^{prac}\right) \tag{10a}$$
$$\text{s.t.}\quad\min_{\|\mathbf{e}_{s,k}\|\le\varepsilon_{s,k},\|\tilde{\mathbf{e}}_{s,k}\|\le\tilde{\varepsilon}_{s,k}}C_{s,k}-\max_{\|\mathbf{E}_{e,l}\|_F\le\varepsilon_{e,l},\|\tilde{\mathbf{E}}_{e,l}\|_F\le\tilde{\varepsilon}_{e,l}}C_{l,k}\ge\bar{R}_s,\forall k, \tag{10b}$$
$$\sum_{k=1}^{K}\mathrm{tr}(\mathbf{F}_k)+\mathrm{tr}(\mathbf{Z})\le P_T,\ \mathrm{tr}(\mathbf{Q})\le P_J, \tag{10c}$$
$$1\ge\rho_{s,k}>0,\ \mathbf{F}_k\succeq\mathbf{0},\ \mathbf{Z}\succeq\mathbf{0},\ \mathbf{Q}\succeq\mathbf{0},\ \mathrm{rank}(\mathbf{F}_k)=1. \tag{10d}$$

A. Problem Formulation

We aim to maximize the minimum harvested power among all CR nodes and EH nodes subject to the secrecy rate constraint, the total transmit power constraint and the CJ power constraint. By taking the above channel model into account, the robust max-min problem can be rewritten as (10) on the top of this page, where $\bar{R}_s$ stands for a given secrecy rate threshold, and P_T and P_J denote the available power budget at the transmitter and the CJ, respectively.

B. Low-Complexity SPCA Algorithm

In this section, we consider an reformulation of problem (10) based on the SPCA method [27]. The optimization framework can also be obtained as a convex form by incorporating channel uncertainties. First, the robust secrecy rate constraint (10b) can be relaxed as

$$C_{s,k}-\log_2\left(1+\frac{\mathrm{tr}\left(\mathbf{H}_{e,l}^H\mathbf{F}_k\mathbf{H}_{e,l}\right)}{\sigma_{e,l}^2+\mathrm{tr}\left(\mathbf{H}_{e,l}^H\mathbf{Z}\mathbf{H}_{e,l}+\mathbf{G}_{e,l}^H\mathbf{Q}\mathbf{G}_{e,l}\right)}\right)\ge\bar{R}_s, \tag{11}$$

Then, (11) can be rewritten as

$$r_1r_2\ge2^{\bar{R}_s}, \tag{12a}$$
$$\frac{\mathbf{h}_{s,k}^H\mathbf{F}_k\mathbf{h}_{s,k}}{\sigma_{s,k}^2+\sum_{j\neq k}\mathbf{h}_{s,k}^H\mathbf{W}_j\mathbf{h}_{s,k}+\mathbf{h}_{s,k}^H\mathbf{Z}\mathbf{h}_{s,k}+\mathbf{g}_{s,k}^H\mathbf{Q}\mathbf{g}_{s,k}+\frac{\sigma_{p,k}^2}{\rho_{s,k}}}\ge r_1-1,\forall l, \tag{12b}$$
$$\frac{\sigma_{e,l}^2+\mathrm{tr}\left(\mathbf{H}_{e,l}^H\mathbf{Z}\mathbf{H}_{e,l}+\mathbf{G}_{e,l}^H\mathbf{Q}\mathbf{G}_{e,l}\right)}{\sigma_{e,l}^2+\mathrm{tr}\left(\mathbf{H}_{e,l}^H(\mathbf{Z}+\mathbf{F}_k)\mathbf{H}_{e,l}+\mathbf{G}_{e,l}^H\mathbf{Q}\mathbf{G}_{e,l}\right)}\ge r_2,\forall k. \tag{12c}$$

where $r_1>0$ and $r_2>0$ are slack variables. (12a) can be transformed into a second-order cone (SOC) form as

$$\left\|\left[\sqrt{2^{\bar{R}_s+2}}\quad r_1-r_2\right]\right\|\le r_1+r_2. \tag{13}$$

Let us define $\bar{\mathbf{H}}_{s,k}\triangleq\bar{\mathbf{h}}_{s,k}\bar{\mathbf{h}}_{s,k}^H$, $\bar{\mathbf{G}}_{s,k}\triangleq\bar{\mathbf{g}}_{s,k}\bar{\mathbf{g}}_{s,k}^H$, $\hat{\mathbf{H}}_{e,l}\triangleq\bar{\mathbf{H}}_{e,l}\bar{\mathbf{H}}_{e,l}^H$, $\hat{\mathbf{G}}_{e,l}\triangleq\bar{\mathbf{G}}_{e,l}\bar{\mathbf{G}}_{e,l}^H$, $\mathbf{H}_{\mathbf{\Delta}_s,k}\triangleq\bar{\mathbf{H}}_{s,k}+\mathbf{\Delta}_{s,k}$, $\mathbf{G}_{\mathbf{\Phi}_s,k}\triangleq\bar{\mathbf{G}}_{s,k}+\mathbf{\Phi}_{s,k}$, $\mathbf{H}_{\mathbf{\Delta}_e,l}\triangleq\hat{\mathbf{H}}_{e,l}+\mathbf{\Delta}_{e,l}$, and $\mathbf{G}_{\mathbf{\Phi}_e,l}\triangleq\hat{\mathbf{G}}_{e,l}+\mathbf{\Phi}_{e,l}$ where $\mathbf{\Delta}_{s,k}=\bar{\mathbf{h}}_{s,k}\mathbf{e}_{s,k}^H+\mathbf{e}_{s,k}\bar{\mathbf{h}}_{s,k}^H+\mathbf{e}_{s,k}\mathbf{e}_{s,k}^H$, $\mathbf{\Phi}_{s,k}=\bar{\mathbf{g}}_{s,k}\tilde{\mathbf{e}}_{s,k}^H+\tilde{\mathbf{e}}_{s,k}\bar{\mathbf{g}}_{s,k}^H+\tilde{\mathbf{e}}_{s,k}\tilde{\mathbf{e}}_{s,k}^H$, $\mathbf{\Delta}_{e,l}=\bar{\mathbf{H}}_{e,l}\mathbf{E}_{e,l}^H+\mathbf{E}_{e,l}\bar{\mathbf{H}}_{e,l}^H+\mathbf{E}_{e,l}\mathbf{E}_{e,l}^H$, and $\mathbf{\Phi}_{e,l}=\bar{\mathbf{G}}_{e,l}\tilde{\mathbf{E}}_{e,l}^H+\tilde{\mathbf{E}}_{e,l}\bar{\mathbf{G}}_{e,l}^H+\tilde{\mathbf{E}}_{e,l}\tilde{\mathbf{E}}_{e,l}^H$, which stand for the CSI uncertainties. Then, the inequalities in (12b) and (12c) can be rearranged, respectively, as

$$\sigma_{s,k}^2+\sum_{j\neq k}\mathbf{w}_j^H\mathbf{H}_{\mathbf{\Delta}_s,k}\mathbf{w}_j+\mathbf{z}^H\mathbf{H}_{\mathbf{\Delta}_s,k}\mathbf{z}+\mathbf{q}^H\mathbf{G}_{\mathbf{\Phi}_s,k}\mathbf{q}+\frac{\sigma_{p,k}^2}{\rho_{s,k}}\le\frac{\mathbf{f}_k^H\mathbf{H}_{\mathbf{\Delta}_s,k}\mathbf{f}_k}{r_1-1},\forall k, \tag{14a}$$
$$\sigma_{e,l}^2+\mathbf{z}^H\mathbf{H}_{\mathbf{\Delta}_e,l}\mathbf{z}+\mathbf{w}_k^H\mathbf{H}_{\mathbf{\Delta}_e,l}\mathbf{w}_k+\mathbf{q}^H\mathbf{G}_{\mathbf{\Phi}_e,l}\mathbf{q}\le\frac{\sigma_{e,l}^2+\mathbf{z}^H\mathbf{H}_{\mathbf{\Delta}_e,l}\mathbf{z}+\mathbf{q}^H\mathbf{G}_{\mathbf{\Phi}_e,l}\mathbf{q}}{r_2},\forall l. \tag{14b}$$

It is straightforward to show that

$$\|\mathbf{\Delta}_{s,k}\|_F\le\|\bar{\mathbf{h}}_{s,k}\mathbf{e}_{s,k}^H\|_F+\|\mathbf{e}_{s,k}\bar{\mathbf{h}}_{s,k}^H\|_F+\|\mathbf{e}_{s,k}\mathbf{e}_{s,k}^H\|_F=\varepsilon_{s,k}^2+2\varepsilon_{s,k}\|\bar{\mathbf{h}}_{s,k}\|\triangleq\xi_{s,k}, \tag{15}$$
$$\|\mathbf{\Phi}_{s,k}\|_F\le\|\bar{\mathbf{g}}_{s,k}\tilde{\mathbf{e}}_{s,k}^H\|_F+\|\tilde{\mathbf{e}}_{s,k}\bar{\mathbf{g}}_{s,k}^H\|_F+\|\tilde{\mathbf{e}}_{s,k}\tilde{\mathbf{e}}_{s,k}^H\|_F=\tilde{\varepsilon}_{s,k}^2+2\tilde{\varepsilon}_{s,k}\|\bar{\mathbf{g}}_{s,k}\|\triangleq\tilde{\xi}_{s,k}, \tag{16}$$
$$\|\mathbf{\Delta}_{e,l}\|_F\le\|\bar{\mathbf{H}}_{e,l}\mathbf{E}_{e,l}^H\|_F+\|\mathbf{E}_{e,l}\bar{\mathbf{H}}_{e,l}^H\|_F+\|\mathbf{E}_{e,l}\mathbf{E}_{e,l}^H\|_F=\varepsilon_{e,l}^2+2\varepsilon_{e,l}\|\bar{\mathbf{H}}_{e,l}\|_F\triangleq\xi_{e,l}, \tag{17}$$
$$\|\mathbf{\Phi}_{e,l}\|_F\le\|\bar{\mathbf{G}}_{e,l}\tilde{\mathbf{E}}_{e,l}^H\|_F+\|\tilde{\mathbf{E}}_{e,l}\bar{\mathbf{G}}_{e,l}^H\|_F+\|\tilde{\mathbf{E}}_{e,l}\tilde{\mathbf{E}}_{e,l}^H\|_F=\tilde{\varepsilon}_{e,l}^2+2\tilde{\varepsilon}_{e,l}\|\bar{\mathbf{G}}_{e,l}\|_F\triangleq\tilde{\xi}_{e,l}. \tag{18}$$

It is noted that $\mathbf{\Delta}_{s,k}$, $\mathbf{\Phi}_{s,k}$, $\mathbf{\Delta}_{e,l}$, and $\mathbf{\Phi}_{e,l}$ are norm-bounded matrices.

According to the results in [26], we can minimize constraint (12b) by minimizing the right-hand side (RHS) of (14a) while maximizing its left-hand side (LHS). Then (14a) and (14b) can be approximately reformulated, respectively, as

$$\max_{\|\Delta_{s,k}\|_F\le\xi_{s,k},\|\Phi_{s,k}\|_F\le\tilde{\xi}_{s,k}}\sigma_{s,k}^2+\sum_{j\neq k}\mathbf{w}_j^H\mathbf{H}_{\mathbf{\Delta}_s,k}\mathbf{w}_j+\mathbf{z}^H\mathbf{H}_{\mathbf{\Delta}_s,k}\mathbf{z}+\mathbf{q}^H\mathbf{G}_{\mathbf{\Phi}_s,k}\mathbf{q}+\frac{\sigma_{p,k}^2}{\rho_{s,k}}\le\min_{\|\Delta_{s,k}\|_F\le\xi_{s,k}}\frac{\mathbf{f}_k^H\mathbf{H}_{\mathbf{\Delta}_s,k}\mathbf{f}_k}{r_1-1},\forall k, \tag{19}$$

$$\max_{\|\Delta_{e,l}\|_F\le\xi_{e,l},\|\Phi_{e,l}\|_F\le\tilde{\xi}_{e,l}} \sigma_{e,l}^2+\mathbf{z}^H\mathbf{H}_{\mathbf{\Delta}_e,l}\mathbf{z} +\mathbf{w}_k^H\mathbf{H}_{\mathbf{\Delta}_e,l}\mathbf{w}_k+\mathbf{q}^H\mathbf{G}_{\mathbf{\Phi}_e,l}\mathbf{q}\le \min_{\|\Delta_{e,l}\|_F\le\xi_{e,l},\|\Phi_{e,l}\|_F\le\tilde{\xi}_{e,l}} \frac{\sigma_{e,l}^2+\mathbf{z}^H\mathbf{H}_{\mathbf{\Delta}_e,l}\mathbf{z}+\mathbf{q}^H\mathbf{G}_{\mathbf{\Phi}_e,l}\mathbf{q}}{r_2},\forall l. \tag{20}$$

Then, a loose approximation method [26] can be utilized to minimize the RHS of (19) and (20) as

$$\begin{aligned}\min_{\|\Delta_{s,k}\|_F\le\xi_{s,k}} \frac{\mathbf{f}_k^H\mathbf{H}_{\mathbf{\Delta}_s,k}\mathbf{f}_k}{r_1-1} &\ge \frac{\mathbf{f}_k^H\bar{\mathbf{H}}_{\xi_s,k}\mathbf{f}_k}{r_1-1},\forall k,\\ \min_{\|\Delta_{e,l}\|_F\le\xi_{e,l},\|\Phi_{e,l}\|_F\le\tilde{\xi}_{e,l}} \frac{\sigma_{e,l}^2+\mathbf{z}^H\mathbf{H}_{\mathbf{\Delta}_e,l}\mathbf{z}+\mathbf{q}^H\mathbf{G}_{\mathbf{\Phi}_e,l}\mathbf{q}}{r_2} &\\ \ge \frac{\sigma_{e,l}^2+\mathbf{z}^H\hat{\mathbf{H}}_{\xi_e,l}\mathbf{z}+\mathbf{q}^H\hat{\mathbf{G}}_{\tilde{\xi}_e,l}\mathbf{q}}{r_2},&\end{aligned} \tag{21}$$

where $\bar{\mathbf{H}}_{\xi_s,k}=\bar{\mathbf{H}}_{s,k}-\xi_{s,k}\mathbf{I}_{N_T}$, $\hat{\mathbf{H}}_{\xi_e,l}=\hat{\mathbf{H}}_{e,l}-\xi_{e,l}\mathbf{I}_{N_T}$ and $\hat{\mathbf{G}}_{\tilde{\xi}_e,l}=\hat{\mathbf{G}}_{e,l}-\tilde{\xi}_{e,l}\mathbf{I}_{N_J}$. Applying a similar technique to the LHS of (19) and (20), we obtain

$$\begin{aligned}&\max_{\|\Delta_{s,k}\|_F\le\xi_{s,k},\|\Phi_{s,k}\|_F\le\tilde{\xi}_{s,k}} \sigma_{s,k}^2+\sum_{j\ne k}\mathbf{w}_j^H\mathbf{H}_{\mathbf{\Delta}_s,k}\mathbf{w}_j\\ &+\mathbf{z}^H\mathbf{H}_{\mathbf{\Delta}_s,k}\mathbf{z}+\mathbf{q}^H\mathbf{G}_{\mathbf{\Phi}_s,k}\mathbf{q}+\frac{\sigma_{p,k}^2}{\rho_{s,k}}\le\sigma_{s,k}^2\\ &+\sum_{j\ne k}\mathbf{w}_j^H\mathbf{H}_{\xi_s,k}\mathbf{w}_j+\mathbf{z}^H\mathbf{H}_{\xi_s,k}\mathbf{z}+\mathbf{q}^H\mathbf{G}_{\tilde{\xi}_s,k}\mathbf{q}+\frac{\sigma_{p,k}^2}{\rho_{s,k}},\forall k,\end{aligned} \tag{22}$$

$$\begin{aligned}&\max_{\|\Delta_{e,l}\|_F\le\xi_{e,l},\|\Phi_{e,l}\|_F\le\tilde{\xi}_{e,l}} \sigma_{e,l}^2+\mathbf{z}^H\mathbf{H}_{\mathbf{\Delta}_e,l}\mathbf{z}\\ &+\mathbf{w}_k^H\mathbf{H}_{\mathbf{\Delta}_e,l}\mathbf{w}_k+\mathbf{q}^H\mathbf{G}_{\mathbf{\Phi}_e,l}\mathbf{q}\le\ \sigma_{e,l}^2\\ &+\mathbf{z}^H\mathbf{H}_{\xi_e,l}\mathbf{z}+\mathbf{w}_k^H\mathbf{H}_{\xi_e,l}\mathbf{w}_k+\mathbf{q}^H\mathbf{G}_{\tilde{\xi}_e,l}\mathbf{q},\forall l,\end{aligned} \tag{23}$$

where $\mathbf{H}_{\xi_s,k}=\bar{\mathbf{H}}_{s,k}+\xi_{s,k}\mathbf{I}_{N_T}$, $\mathbf{G}_{\tilde{\xi}_s,k}=\bar{\mathbf{G}}_{s,k}+\tilde{\xi}_{s,k}\mathbf{I}_{N_J}$, $\mathbf{H}_{\xi_e,l}=\hat{\mathbf{H}}_{e,l}+\xi_{e,l}\mathbf{I}_{N_T}$, and $\mathbf{G}_{\tilde{\xi}_e,l}=\hat{\mathbf{G}}_{e,l}+\tilde{\xi}_{e,l}\mathbf{I}_{N_J}$.

According to (19)-(23), (14a) and (14b) can be converted respectively as

$$\begin{aligned}&\sigma_{s,k}^2+\sum_{j\ne k}\mathbf{w}_j^H\mathbf{H}_{\xi_s,k}\mathbf{w}_j+\mathbf{z}^H\mathbf{H}_{\xi_s,k}\mathbf{z}+\mathbf{q}^H\mathbf{G}_{\tilde{\xi}_s,k}\mathbf{q}\\ &+\frac{\sigma_{p,k}^2}{\rho_{s,k}}\le\frac{\mathbf{f}_k^H\bar{\mathbf{H}}_{\xi_s,k}\mathbf{f}_k}{r_1-1},\forall k,\end{aligned} \tag{24}$$

$$\begin{aligned}&\sigma_{e,l}^2+\mathbf{z}^H\mathbf{H}_{\xi_e,l}\mathbf{z}+\mathbf{w}_k^H\mathbf{H}_{\xi_e,l}\mathbf{w}_k+\mathbf{q}^H\mathbf{G}_{\tilde{\xi}_e,l}\mathbf{q}\\ &\le\frac{\sigma_{e,l}^2+\mathbf{z}^H\hat{\mathbf{H}}_{\xi_e,l}\mathbf{z}+\mathbf{q}^H\hat{\mathbf{G}}_{\tilde{\xi}_e,l}\mathbf{q}}{r_2},\forall k,l.\end{aligned} \tag{25}$$

It is observed that (24) and (25) are non-convex, while the RHS of both (24) and (25) has a quadratic-over-linear (QoL) form, which is convex [24].

Following the idea of the constrained convex procedure [27], the QoL functions can be replaced by their first-order expansions. By adopting the Taylor expansion in [12], for the points $(\tilde{\mathbf{w}}_k,\tilde{r}_1)$, $(\tilde{\mathbf{z}},\tilde{r}_2)$ and $(\tilde{\mathbf{q}},\tilde{r}_2)$, (24) and (25) are transformed into convex forms, respectively, as

$$\begin{aligned}&\sigma_{s,k}^2+\sum_{j\ne k}\mathbf{w}_j^H\mathbf{H}_{\xi_s,k}\mathbf{w}_j+\mathbf{z}^H\mathbf{H}_{\xi_s,k}\mathbf{z}+\mathbf{q}^H\mathbf{G}_{\tilde{\xi}_s,k}\mathbf{q}+\frac{\sigma_{p,k}^2}{\rho_{s,k}}\\ &\le F_{\bar{\mathbf{H}}_{\xi_s,k},1}(\mathbf{w}_k,r_1,\tilde{\mathbf{w}}_k,\tilde{r}_1),\end{aligned} \tag{26a}$$

$$\begin{aligned}&\sigma_{e,l}^2+\mathbf{z}^H\mathbf{H}_{\xi_e,l}\mathbf{z}+\mathbf{w}_k^H\mathbf{H}_{\xi_e,l}\mathbf{w}_k+\mathbf{q}^H\mathbf{G}_{\tilde{\xi}_e,l}\mathbf{q}\\ &\le\sigma_{e,l}^2(\frac{2}{\tilde{r}_2}-\frac{r_2}{\tilde{r}_2^2})+F_{\hat{\mathbf{H}}_{\xi_e,l},0}(\mathbf{z},r_2,\tilde{\mathbf{z}},\tilde{r}_2)\\ &\quad+F_{\hat{\mathbf{G}}_{\tilde{\xi}_e,l},0}(\mathbf{q},r_2,\tilde{\mathbf{q}},\tilde{r}_2),\forall k,l.\end{aligned} \tag{26b}$$

Following (6), the inverse function of $\Phi^{prac}(P_{in})$ can be written as

$$P_{in}(\Phi^{prac})\triangleq b-\frac{1}{a}\ln\left(\frac{e^{ab}(P_{max}-\Phi^{prac})}{e^{ab}\Phi^{prac}+P_{max}}\right). \tag{27}$$

Then, applying (27), (10a) can be transformed to be

$$\begin{aligned}&\sum_{j=1}^K\mathbf{w}_j^H\bar{\mathbf{H}}_{\xi_s,k}\mathbf{w}_j+\mathbf{z}^H\bar{\mathbf{H}}_{\xi_s,k}\mathbf{z}+\mathbf{q}^H\bar{\mathbf{G}}_{\tilde{\xi}_s,k}\mathbf{q}\\ &\quad\ge\frac{P_{in}(\bar{E}_s)}{1-\rho_{s,k}}-\sigma_{s,k}^2,\forall k,\end{aligned} \tag{28a}$$

$$\begin{aligned}&\mathbf{z}^H\hat{\mathbf{H}}_{\xi_e,l}\mathbf{z}+\sum_{j=1}^K\mathbf{w}_j^H\hat{\mathbf{H}}_{\xi_e,l}\mathbf{w}_j+\mathbf{q}^H\hat{\mathbf{G}}_{\tilde{\xi}_e,l}\mathbf{q}\\ &\quad\ge P_{in}(\bar{E}_e)-N_E\sigma_{e,l}^2,\forall l,\end{aligned} \tag{28b}$$

where $\bar{\mathbf{G}}_{\tilde{\xi}_s,k}=\bar{\mathbf{G}}_{s,k}+\tilde{\xi}_{s,k}\mathbf{I}$. Substituting $\mathbf{w}_j\triangleq\tilde{\mathbf{w}}_j+\Delta\mathbf{w}_j$, $\mathbf{z}\triangleq\tilde{\mathbf{z}}+\Delta\mathbf{z}$, and $\mathbf{q}\triangleq\tilde{\mathbf{q}}+\Delta\mathbf{q}$ into the LHS of (28a), we get

$$\begin{aligned}&\sum_{j=1}^K\mathbf{w}_j^H\bar{\mathbf{H}}_{\xi_s,k}\mathbf{w}_j+\mathbf{z}^H\bar{\mathbf{H}}_{\xi_s,k}\mathbf{z}+\mathbf{q}^H\bar{\mathbf{G}}_{\tilde{\xi}_s,k}\mathbf{q}\\ &\ge\sum_{j=1}^K\left(\tilde{\mathbf{w}}_j^H\bar{\mathbf{H}}_{\xi_s,k}\tilde{\mathbf{w}}_j+2\Re\{\tilde{\mathbf{w}}_j^H\bar{\mathbf{H}}_{\xi_s,k}\Delta\mathbf{w}_j\}\right)+\tilde{\mathbf{z}}^H\bar{\mathbf{H}}_{\xi_s,k}\tilde{\mathbf{z}}\\ &\quad+\tilde{\mathbf{q}}^H\bar{\mathbf{G}}_{\tilde{\xi}_s,k}\tilde{\mathbf{q}}+2\Re\{\tilde{\mathbf{z}}^H\bar{\mathbf{H}}_{\xi_s,k}\Delta\mathbf{z}+\tilde{\mathbf{q}}^H\bar{\mathbf{G}}_{\tilde{\xi}_s,k}\Delta\mathbf{q}\},\end{aligned} \tag{29}$$

where the inequality is obtained by dropping the quadratic terms $\Delta\mathbf{w}_j^H\bar{\mathbf{H}}_{\xi_s,k}\Delta\mathbf{w}_j$, $\Delta\mathbf{z}^H\bar{\mathbf{H}}_{\xi_s,k}\Delta\mathbf{z}$ and $\Delta\mathbf{q}^H\bar{\mathbf{G}}_{\tilde{\xi}_s,k}\Delta\mathbf{q}$.

Similarly, the LHS of (28b) can be derived as

$$\begin{aligned}&\tilde{\mathbf{z}}^H\hat{\mathbf{H}}_{\xi_e,l}\tilde{\mathbf{z}}+\tilde{\mathbf{q}}^H\hat{\mathbf{G}}_{\tilde{\xi}_e,l}\tilde{\mathbf{q}}+2\Re\{\tilde{\mathbf{z}}^H\hat{\mathbf{H}}_{\xi_e,l}\Delta\mathbf{z}+\tilde{\mathbf{q}}^H\hat{\mathbf{G}}_{\tilde{\xi}_e,l}\Delta\mathbf{q}\}+\\ &\sum_{j=1}^K\left(\tilde{\mathbf{w}}_j^H\hat{\mathbf{H}}_{\xi_e,l}\tilde{\mathbf{w}}_j+2\Re\{\tilde{\mathbf{w}}_j^H\hat{\mathbf{H}}_{\xi_e,l}\Delta\mathbf{w}_j\}\right)\ge P_{in}(\bar{E}_e)-N_E\sigma_{e,l}^2.\end{aligned} \tag{30}$$

It is noted that (28a) is still non-convex in its current form since it involves coupled $\bar{E}_s$ and $1-\rho_{s,k}$. By defining $a_{s,k}\triangleq\sum_{j=1}^K\left(\tilde{\mathbf{w}}_j^H\bar{\mathbf{H}}_{\xi_s,k}\tilde{\mathbf{w}}_j+2\Re\{\tilde{\mathbf{w}}_j^H\bar{\mathbf{H}}_{\xi_s,k}\Delta\mathbf{w}_j\}\right)+\tilde{\mathbf{z}}^H\bar{\mathbf{H}}_{\xi_s,k}\tilde{\mathbf{z}}+2\Re\{\tilde{\mathbf{z}}^H\bar{\mathbf{H}}_{\xi_s,k}\Delta\mathbf{z}+\tilde{\mathbf{q}}^H\bar{\mathbf{G}}_{\tilde{\xi}_s,k}\Delta\mathbf{q}\}+\tilde{\mathbf{q}}^H\bar{\mathbf{G}}_{\tilde{\xi}_s,k}\tilde{\mathbf{q}}+\sigma_{s,k}^2$, (28a) can be rewritten as

$$a_{s,k}(1-\rho_{s,k})\ge P_{in}(\bar{E}_s),\forall k. \tag{31}$$

Based on a first-order Taylor approximation of $P_{in}(\bar{E}_s)$, (31) can be recast as the SOC constraint

$$\left\|\left[2e_s \quad a_{s,k}+\rho_{s,k}-1\right]\right\| \le a_{s,k}-\rho_{s,k}+1, \tag{32}$$

where $e_s = P_{in}(\tilde{E}_s)+P'_{in}(\tilde{E}_s)(\bar{E}_s-\tilde{E}_s)$.

In addition, (10c) can be reformulated as two SOC forms

$$\left\|\left[\mathbf{w}_1^T \quad \ldots \quad \mathbf{w}_K^T \quad \mathbf{z}^T\right]\right\| \le \sqrt{P_T}, \tag{33a}$$

$$\left\|\mathbf{q}^T\right\| \le \sqrt{P_J}. \tag{33b}$$

Now we propose a new algorithm based on the SPCA method [27], which iteratively optimizes $\left\{\tilde{\mathbf{F}}_k, \tilde{\mathbf{q}}, \tilde{\mathbf{z}}, \tilde{r}_1, \tilde{r}_2, \tilde{E}_s\right\}$. Let us denote $\Psi^{(n)} = \left\{\tilde{\mathbf{w}}_k^{(n)}, \tilde{\mathbf{q}}^{(n)}, \tilde{\mathbf{z}}^{(n)}, \tilde{r}_1^{(n)}, \tilde{r}_2^{(n)}, \tilde{E}_s^{(n)}\right\}$ as the optimal solution obtained at the n-th iteration. At the $(n+1)$-th iteration, given $\Psi^{(n)}$, problem (10) is converted into the convex form as

$$\begin{aligned} \max_{\rho_{s,k},\{\mathbf{f}_k\},\mathbf{z},\mathbf{q},\bar{E}_s,\bar{E}_e,\,r_1,r_2} \quad & \bar{E}_s+\bar{E}_e \\ \text{s.t.} \quad & (13),\,(26a),\,(26b),\,(30),\,(32),\,(33a),\,(33b), \\ & 0<\rho_{s,k}\le 1, \quad \Delta\mathbf{z}=\mathbf{z}-\tilde{\mathbf{z}}^{(n)}, \\ & \Delta\mathbf{q}=\mathbf{q}-\tilde{\mathbf{q}}^{(n)},\, \Delta\mathbf{w}_k=\mathbf{w}_k-\tilde{\mathbf{w}}_k^{(n)}, \forall k. \end{aligned} \tag{34}$$

Problem (34) is a SOCP problem [24], which can be solved by employing the CVX tools [25].

IV. Simulation Results

In this section, we provide the simulation results to validate the performance of our proposed scheme. The system parameters that we have considered for the simulations are summarized in Table I, where Tx means the transmitter. The estimated channel $\overline{\mathbf{h}}_{s,k}$, $\overline{\mathbf{H}}_{e,l}$,$\overline{\mathbf{g}}_{s,k}$, and $\overline{\mathbf{G}}_{e,l}$ are respectively modelled as $\overline{\mathbf{h}}_{s,k}=H(d_{s,k})\overline{\mathbf{h}}_I$, $\overline{\mathbf{H}}_{e,l} = H(d_{e,l})\overline{\mathbf{H}}_I$, $\overline{\mathbf{g}}_{s,k} = H(f_{s,k})\overline{\mathbf{g}}_I$, and $\overline{\mathbf{G}}_{e,l} = H(f_{e,l})\overline{\mathbf{G}}_I$, where $H(d) = \frac{c}{4\pi f_c}(\frac{1}{d})^{\frac{\kappa}{2}}$, $\overline{\mathbf{h}}_I \sim \mathcal{CN}(0,\mathbf{I})$, $\overline{\mathbf{H}}_I \sim \mathcal{CN}(0,\mathbf{I})$, $\overline{\mathbf{g}}_{s,k} \sim \mathcal{CN}(0,\mathbf{I})$, and $\overline{\mathbf{G}}_{e,l} \sim \mathcal{CN}(0,\mathbf{I})$. We fix the channel error bound for the deterministic model as $\varepsilon_s = \varepsilon_{s,k} = \tilde{\varepsilon}_{s,k}, \forall k$ and $\varepsilon_e = \varepsilon_{e,l} = \tilde{\varepsilon}_{e,l}, \forall k$. For the non-linear EH model, we set $M = M_{s,k} = M_{e,l} = 3.9$ mW, $a = a_{s,k} = a_{e,l} = 1500$ and $b = b_{s,k} = b_{e,l} = 0.0022$ according to the measurement data results [22]. In our simulations, we compare the no-AN scheme which is obtained by setting $\mathbf{Q}_m = \mathbf{0}, \forall m$, no-CJ scheme which is computed by $\mathbf{Z} = \mathbf{0}$ [13], and the non-robust method which assumes no uncertainty in the CSI [13].

Fig. 2 illustrates the convergence of the SOCP-SPCA method with respect to the iteration numbers for $P_T = 40$ dBm, $P_J = 40$ dBm, $\bar{R}_s = 0.5$ bps/Hz, and $\varepsilon = 0.01$. We can see that the convergence of the SOCP-SPCA method is achieved for all cases within just 5 iterations.

Fig. 3 shows the average harvested energy in terms of different target secrecy rates with $P_T = 30$ dBm and $P_J = 30$ dBm. Here, "SOCP-SPCA" denote our proposed schemes, while "no-AN", "no-CJ" and "no-robust" represent the benchmark designs. It is observed that the harvested power of all schemes declines with the increased secrecy rate target.

TABLE I
System Parameters

Number of CR node, K	2
Number of EH node, L	2
Number of CJ node antenna, N_J	4
Number of EH node antenna, N_E	2
Number of transmitter antenna, N_T	4
Distance between the Tx and the CR node, $d_{s,k}$	10 m
Distance between the CJ and the CR node, $f_{s,k}$	10 m
Distance between the Tx and the EH node, $d_{e,l}$	5 m
Distance between the CJ and the EH node, $f_{e,l}$	5 m
Carrier frequency, f_c	900 MHz
Path loss exponent, κ	2.7
Noise power at the CR nodes, $\sigma_{s,k}^2$	-90 dBm
Noise power at the CR nodes, $\sigma_{p,k}^2$	-50 dBm
Noise power of all the EH nodes, σ_k^2	-90 dBm

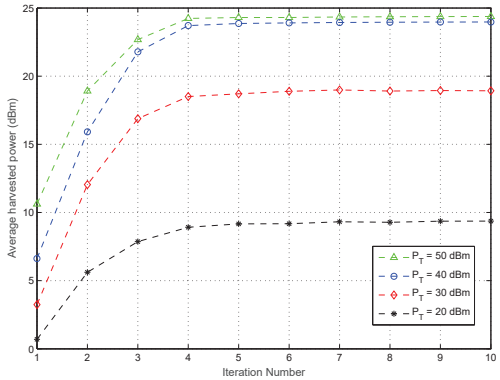

Fig. 2. Average harvested energy with respect to the iteration numbers for the SPCA method

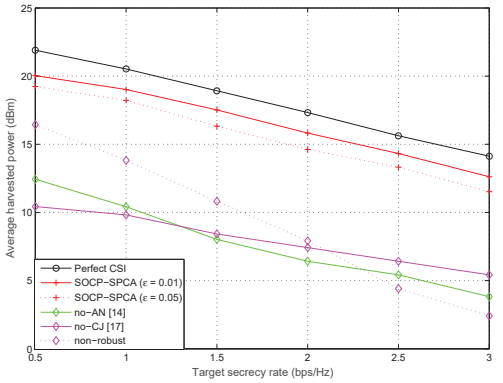

Fig. 3. Average harvested energy with respect to the target secrecy rate

Compared with the no-AN scheme and the no-CJ scheme, the harvested power of the SOCP-SPCA algorithm is 9 dB and 8 dB higher, respectively. Moreover, we can check that the proposed algorithm outperforms the non-robust scheme, and the performance gap increases as the target secrecy rate becomes large.

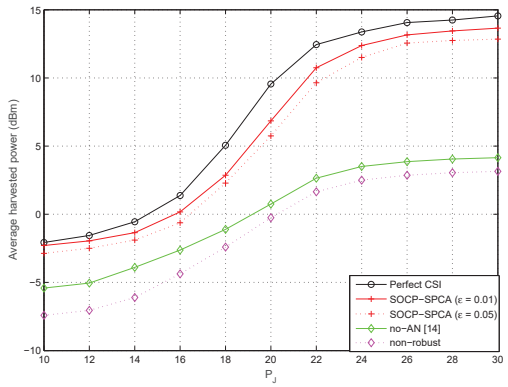

Fig. 4. Average harvested energy with respect to the power budget at the CJ

Fig. 4 depicts the average harvested energy in terms of the power budget at the CJ with $P_T = 10$ dBm and $\bar{R}_s = 0.5$ bps/Hz. It is easily observed that the achieved harvested power grows with P_J. We can check that as P_J increases, the performance gap between the proposed SOCP-SPCA algorithm and the no-AN scheme becomes larger and a performance loss of the non-robust scheme grows.

V. Conclusion

In this paper, we have studied robust secure beamforming designs for a power splitting MIMO SWIPT IoT network under a non-Linear EH model with coopertive jamming, where norm-bounded channel uncertainties are present. By incorporating a norm-bounded channel uncertainty model, we propose an algorithm based on SPCA, which will reduce computational complexity. Finally, simulation results have shown that the proposed robust design outperforms conventional schemes reported in the literature. The proposed robust secrecy design framework and solution approach have potentials to be extended to more complex SWIPT systems by incorporating new security strategies.

References

[1] C. X. Wang *et al.*, "Cellular architecture and key technologies for 5G wireless communication networks," *IEEE Commun. Mag.*, vol. 52, no. 2, pp. 122-130, Feb. 2014.

[2] R. Zhang and C. Ho, "MIMO broadcasting for simultaneous wireless information and power transfer," *IEEE Trans. Wireless Commun.*, vol. 12, no. 5, pp. 1989-2001, May 2013.

[3] J. Tang, D. K. C. So, N. Zhao, A. Shojaeifard, and K.-K. Wong, "Energy efficiency optimization with SWIPT in MIMO broadcast channels for Internet of Things," *IEEE Internet of Things J.*, vol. 5, no. 4, Aug. 2018.

[4] Y. Huang, M. Liu, and Y. Liu, "Energy-Efficient SWIPT in IoT Distributed Antenna Systems," *IEEE Internet of Things J.*, vol. 5, no. 4, pp. 2646-2656, Aug. 2018.

[5] Y. Hu, Y. Zhu, M. C. Gursoy, and A. Schmeink, "SWIPT-enabled relaying in IoT networks operating with finite blocklength codes," *IEEE J. Sel. Areas Commun.*, vol. 37, no. 1, pp. 74-88, Jan. 2019.

[6] D. Mishra, G. C. Alexandropoulos and S. De, "Energy sustainable IoT with individual QoS constraints through MISO SWIPT multicasting," *IEEE Internet of Things Journal*, vol. 5, no. 4, pp. 2856-2867, Aug. 2018.

[7] S. Goel and R. Negi, "Guaranteeing secrecy using artificial noise," *IEEE Trans. Wireless Commun.*, vol. 7, no. 6, pp. 2180-2189, Jun. 2008.

[8] Z. Zhu, S. Huang, Z. Chu, F. Zhou, D. Zhang and I. Lee, "Robust designs of beamforming and power splitting for distributed antenna systems with wireless energy harvesting," *IEEE Systems Journal.*, vol. 13, no. 1, pp. 30-41, Mar. 2019.

[9] Z. Zhu, Z. Wang, Z. Chu, X. Gao, Y. Zhang, and J. Cui, "Robust beamforming based on transmit power analysis for multiuser multiple-input-single-output interference channels with energy harvesting," *IET Communications*, vol. 10, no. 10, pp. 1221-1228, Jul. 2016.

[10] D. Xu and H. Zhu, "Secure transmission for SWIPT IoT systems with full-duplex IoT devices," *IEEE Internet of Things J.*, vol. 6, no. 6, pp. 10915-10933, Dec. 2019.

[11] Z. Zhu, Z. Chu, Z. Wang, and I. Lee, "Outage constrained robust beamforming for secure broadcasting systems with energy harvesting," *IEEE Transactions on Wireless Communications*, vol. 15, no. 11, pp. 7610-7620, Nov. 2016.

[12] Z. Chu, Z. Zhu, W. Xiang, and J. Hussein, "Robust beamforming and power splitting design in MISO SWIPT downlink system," *IET Commun.*, vol. 10, no. 6, pp. 691-698, Apr. 2016.

[13] Z. Zhu, Z. Chu, N. Wang, S. Huang, Z. Wang, and I. Lee, "Beamforming and power splitting designs for AN-aided secure multi-user MIMO SWIPT systems," *IEEE Trans. Inf. Forensics Security*, vol. 12, no. 12, pp. 2861-2874, Dec. 2017.

[14] Z. Chu, H. Nguyen, T. Le, M. Karamanoglu, E. Ever, and A. Yazici, "Secure wireless powered and cooperative jamming D2D communications," *IEEE Trans. Green Commun. Netw.*, vol. 2, no. 1, pp. 1-13, Mar. 2018.

[15] Z. Zhu, N. Wang, W. Hao, Z. Wang, and I. Lee, "Robust beamforming designs in secure MIMO SWIPT IoT networks with a non-linear channel model," *IEEE Internet of Things Journal*, vol. 8, no. 3, pp. 1702-1715, Aug 2020.

[16] J. Moon, H. Lee, C. Song, and I. Lee, "Secrecy performance optimization for wireless powered communication networks with an energy harvesting jammer," *IEEE Trans. Commun.*, vol. 65, no. 2, pp. 764-774, Feb. 2017.

[17] Z. Chu, T. A. Le, H. X. Nguyen, M. Karamanoglu, Z. Zhu, "Robust design for MISO SWIPT system with artificial noise and cooperative jamming," in *Proc. IEEE GLOBECOM*, pp. 1-6, Dec. 2017.

[18] Z. Zhu, Z. Chu, N. Wang, Z. Wang, and I. Lee, "Energy harvesting fairness in AN-aided secure MU-MIMO SWIPT systems with cooperative jammer," in *Proc. IEEE ICC*, pp. 1-6, May 2018.

[19] R. Jiang, K. Xiong, P. Fan, Y. Zhang, and Z. Zhong, "Power minimization in SWIPT networks with coexisting power-splitting and time-switching users under nonlinear EH model," *IEEE Internet of Things J.*, vol. 6, no. 5, pp. 8853-8869, Oct. 2019.

[20] X. Hu, B. Li, K. Huang, Z. Fei, and K. Wong, "Secrecy energy efficiency in wireless powered heterogeneous networks: A distributed ADMM approach," *IEEE Access*, vol. 6, pp. 20609-20624, 2018.

[21] E. Boshkovska, D. W. K. Ng, N. Zlatanov, and R. Schober, "Practical non-linear energy harvesting model and resource allocation for SWIPT systems," *IEEE Commun. Lett.*, vol. 19, no. 12, pp. 2082-2085, Dec. 2015.

[22] Z. Zhu, Z. Chu, F. Zhou, H. Niu, Z. Wang and I. Lee, "Secure Beamforming Designs for Secrecy MIMO SWIPT Systems," *IEEE Wireless Communications Letters*, vol. 7, no. 3, pp. 424-427, June 2018.

[23] K. B. Petersern and M. S. Pedersern, *The Matrix Cookbook*. Cambridge, MA, USA: MIT Press, Nov. 2008. [Online]. Available: http:// matrixcookbook.com

[24] S. Boyd and L. Vandenberghe, *Convex Optimization*. Cambridge, U.K.: Cambridge Univ. Press, 2004.

[25] M. Grant and S. Boyd, "CVX: Matlab software for disciplined convex programming," Available: http://cvxr.com/cvx, Sep. 2012.

[26] M. Bengtsson and B. Ottersten, "Optimum and suboptimum transmit beamforming," *Handbook of Antennas in Wireless Communications,* L. C. Godara, Ed., CRC Press, Aug. 2001.

[27] A. S. Vishwanathan, A. J. Smola, and S. V. N. Vishwanathan, "Kernel methods for missing variables," in Proc. *Int. Workshop Artif. Intell. Stat.*, pp. 325-332, Jan. 2005.